Quantum-Hall Activation Gaps in Graphene

A. J. M. Giesbers,[1,*] U. Zeitler,[1,†] M. I. Katsnelson,[2] L. A. Ponomarenko,[3] T. M. Mohiuddin,[3] and J. C. Maan[1]

[1]*High Field Magnet Laboratory, Institute for Molecules and Materials, Radboud University Nijmegen, Toernooiveld 7, 6525 ED Nijmegen, The Netherlands*

[2]*Condensed Matter Theory, Institute for Molecules and Materials, Radboud University Nijmegen, Toernooiveld 1, 6525 ED Nijmegen, The Netherlands*

[3]*Department of Physics, University of Manchester, M13 9PL, Manchester, United Kingdom*

(Received 18 April 2007; published 14 November 2007)

We have measured the quantum-Hall activation gaps in graphene at filling factors $\nu = 2$ and $\nu = 6$ for magnetic fields up to 32 T and temperatures from 4 to 300 K. The $\nu = 6$ gap can be described by thermal excitation to broadened Landau levels with a width of 400 K. In contrast, the gap measured at $\nu = 2$ is strongly temperature and field dependent and approaches the expected value for sharp Landau levels for fields $B > 20$ T and temperatures $T > 100$ K. We explain this surprising behavior by a narrowing of the lowest Landau level.

DOI: 10.1103/PhysRevLett.99.206803 PACS numbers: 73.43.−f, 71.70.Di, 73.63.−b

The quantum-Hall effect (QHE) observed in two-dimensional electron systems (2DESs) is one of the fundamental quantum phenomena in solid state physics. Since its discovery in 1980 [1] it has been important for fundamental physics [2] and application to quantum metrology [3]. Recently a new member joined the family of 2DESs: graphene, a single layer of carbon atoms [4–8]. Graphene displays a unique charge carrier spectrum of chiral Dirac fermions [9,10] and enriches the QHE with a half integer QHE of massless relativistic particles observed in single-layer graphene [11–14] and a novel type of integer QHE of massive chiral fermions in bilayers [15,16]. Moreover, the band structure of graphene even allows the observation of the QHE up to room temperature [17]. Since localization in conventional quantum-Hall systems is already fully destroyed at moderate temperatures, no QHE has been observed at temperatures above 30 K until very recently. Therefore, understanding a room temperature QHE in graphene goes far beyond our comprehension of the traditional QHE.

In order to access this intriguing phenomenon in more detail, we report here systematic measurements of the inter-Landau-level activation gap in graphene for magnetic fields up to 32 T. We will show that the gap between the zeroth and the first Landau level approaches the bare, unbroadened Landau-level separation for high magnetic fields and we explain these findings by a much narrower lowest Landau-level compared to the other ones. In contrast, for higher Landau levels, the measured activation gap behaves as expected for equally broadened states.

The single-layer graphene samples [Fig. 1(c)] were made by the micromechanical exfoliation of crystals of natural graphite, followed by the selection of single-layer flakes using optical microscopy and atomic force microscopy [4,5]. A large enough single-layer flake is contacted by Au electrodes and patterned into a Hall bar by e-beam lithography with subsequent reactive plasma etching. The structures are deposited on a SIMOX substrate with a 300 nm thick SiO_2 layer on top of heavily doped Si. The Si is used as a backgate allowing to tune the carrier concentration n to either holes ($n < 0$) or electrons ($n > 0$) with a mobility $\mu = 15\,000\ \mathrm{cm}^2(\mathrm{V\,s})^{-1}$ at 4.2 K. Because of the presence of surface impurities on the graphene sheet [18], the devices are generally strongly hole doped with a charge neutrality point situated at a positive back-gate voltage. In order to restore a pristine undoped situation we anneal our samples at 390 K during several hours prior to any experiment, thereby removing most of the impurities and placing the charge neutrality point as close as possible to zero gate voltage [7].

Electrons in graphene behave as chiral Dirac fermions with a linear dispersion $E = c\hbar|k|$, where $c \approx 10^6\ \mathrm{ms}^{-1}$ is the electron velocity [10]. In a magnetic field the energy spectrum splits up into nonequidistant Landau levels [Fig. 1(a)] with energies given by [11–14].

$$E_N = \mathrm{sgn}\,(N)\sqrt{2\hbar c^2 eB|N|}. \quad (1)$$

N is a negative integer value for holes and positive for electrons. The $N = 0$ Landau level is shared equally between both carrier types.

In Fig. 1(b) we have plotted the Hall resistivity ρ_{xy} as a function of the magnetic field for a hole-doped device ($n = -1.0 \times 10^{12}\ \mathrm{cm}^{-2}$) at $T = 4.2$ K and at room temperature (RT). At 4.2 K pronounced plateaus, accompanied by zero longitudinal resistivity, are visible in ρ_{xy} at values of $\rho_{xy} = -h/e^2\nu$, with $\nu = -2$ and $\nu = -6$. At $B \approx 21$ T ($\nu = -2$) the Fermi energy is situated on the localized states between the zeroth ($N = 0$) and first ($N = -1$) Landau level of the holes [see Fig. 1(a)]. All levels below the Fermi energy are now completely filled and ρ_{xy} is quantized to $h/2e^2$. When sweeping the magnetic field downwards more Landau levels become populated and $\nu = -6$ is reached at $B \approx 7$ T. The Fermi energy now lies between the first ($N = -1$) and the second ($N = -2$) Landau level and ρ_{xy} is quantized at $h/6e^2$.

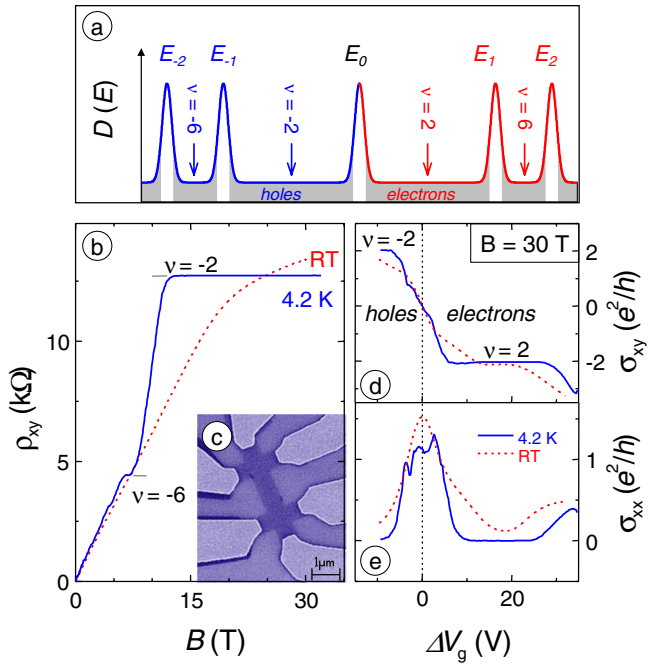

FIG. 1 (color online). (a) Schematic Landau-level structure in graphene. The white areas are extended states in the center of the Landau levels, with the localization radius of order of the sample size; the gray areas represent localized states in between. The arrows indicate the position of the chemical potential for the corresponding filling factor. (b) Hall resistivity ρ_{xy} for holes in a single-layer graphene device as a function of the magnetic field. The traces were recorded at 4.2 K (blue, solid line) and RT (red, dashed line) at a fixed gate voltage corresponding to a carrier concentration $n = -1.0 \times 10^{12}$ cm^{-2}. (c) Scanning electron micrograph of the graphene multiterminal device. Hall conductivity σ_{xy} (d) and conductivity σ_{xx} (e) at 4.2 K (blue, solid line) and at RT (red, dashed line) as a function of the gate voltage at $B = 30$ T.

The quantization of the Hall resistance, especially at room temperature, can be seen most clearly by varying the carrier concentration at the highest possible magnetic field. This is shown in Fig. 1(d) and 1(e) for $B = 30$ T, where we plot the Hall conductivity σ_{xy} and the conductivity σ_{xx} as a function of the applied gate voltage at 4.2 K and RT. The conductivity tensor $\boldsymbol{\sigma}$ was calculated by inverting the experimentally measured resistivity tensor $\boldsymbol{\rho}$. The corresponding quantum-Hall plateaus for holes ($\nu = -2$) and electrons ($\nu = 2$), accompanied by minima in σ_{xx}, are quantized to $\sigma_{xy} = \pm 2e^2/h$ and remain visible up to RT.

It is interesting to note that the low-temperature data shown in Fig. 1(e) demonstrate a splitting of the conductivity maximum around the charge neutrality point which disappears at higher temperatures. As reported previously [6,19], this observation may be explained as a Zeeman splitting of the order of a few Kelvin [6] or the presence of counterpropagating edge channels dominating the resistivity ρ_{xx} [19]. Additionally, a spontaneous spin and/or valley polarization due to $SU(4)$ quantum-Hall ferromagnetism was suggested [20], possibly explaining the disappearance of the splitting at higher temperatures with a crossing of the Curie temperature. Whether such a polarization survives up to the high temperatures with a value of the splitting smaller than the thermal energy is still subject of scientific debate and goes beyond the scope of this work. For completely filled Landau levels, however, as we consider in the rest of this Letter, no spontaneous polarization takes place and no interaction induced splitting is expected.

To determine the energy gaps we have measured ρ_{xx} as a function of the carrier concentration at a constant magnetic field (5 to 30 T in steps of 5 T) and at different temperatures between 4.2 K and RT. Typical results for $B = 15$ T are shown in Fig. 2. At this intermediate field all the minima already display a clearly visible temperature dependence. At the highest field (30 T) the $\nu = 2$ minimum remains close to zero for all temperatures [see Fig. 1(e)]. The value of the minima in the longitudinal resistivity starts to deviate from zero with increasing temperature and the quantum-Hall plateaus become less pronounced. Clearly, the $\nu = \pm 2$ minimum is much more robust at higher temperatures than the $\nu = 6$ minimum, which is also the case for the related quantum-Hall plateaus.

The value of the resistance minima at $\nu = 2$ and $\nu = 6$ as a function of the inverse temperature for different magnetic fields are shown in Fig. 3(a) and 3(b), respectively [21]. From the slope in these Arrhenius plots,

$$\rho_{xx} \propto \exp(-\Delta_a/kT), \tag{2}$$

we deduce the activation gap Δ_a. All data for $T \geq 100$ K

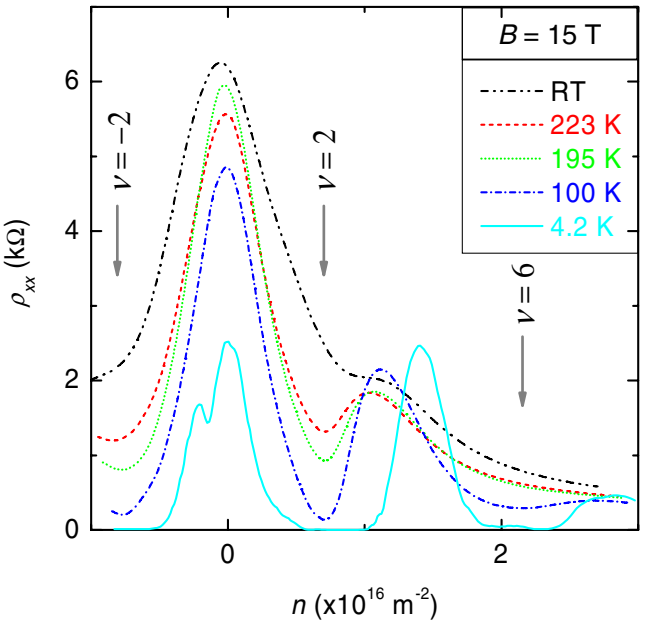

FIG. 2 (color online). Resistivity ρ_{xx} as a function of carrier concentration at $B = 15$ T for different temperatures. The arrows mark the $\nu = \pm 2$ and the $\nu = 6$ minima.

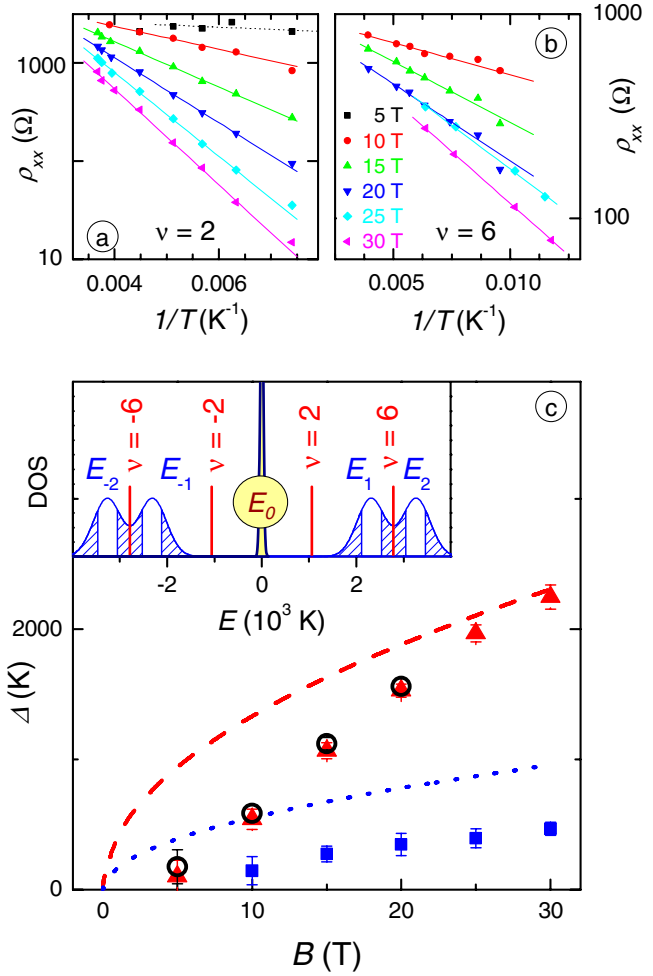

FIG. 3 (color online). Arrhenius plots of ρ_{xx} in the high temperature range for the gaps at $\nu = 2$ (a) and at $\nu = 6$ (b) for different magnetic fields. (c) Energy gaps $2\Delta_a$ between two Landau levels as a function of magnetic field for $\nu = +2$ (full red triangles), $\nu = -2$ (open black circles), and $\nu = 6$ (full blue squares) as deduced from the Arrhenius plots. The dashed (red) and dotted (blue) lines are the theoretically expected energy gaps for sharp Landau levels. The inset shows schematically the density of states for a sharp zeroth Landau level and broadened higher Landau levels for electrons and holes at 30 T. The form and width of the higher Landau levels were extracted from experimental data. Extended states are represented by the white areas, localized states by the dashed areas.

can be reasonably fitted with a single Arrhenius exponent. For $T < 100$ K, in particular, for $\nu = \pm 2$, the Arrhenius plots flatten off significantly, an effect normally attributed to variable-range hopping [22,23].

In Fig. 3(c) we show the results of the measured gaps and compare them to the bare Landau-level separation as given by Eq. (1). Gaps for $\nu = -2$ were obtained using a similar Arrhenius analysis as in Fig. 3(a), yielding very comparable results as for the gaps at $\nu = +2$. However, due to a leakage current through the gate insulator for too negative gate voltages, $\nu = -2$ moves beyond experimental reach for $B > 20$ T.

The experimental values for $\nu = 6$ show a constant offset of ~400 K from the ideal curve, which can straightforwardly be explained by a corresponding finite Landau-level width [24].

In contrast, the $\nu = \pm 2$ gap behaves strikingly different. At low magnetic fields a lower value than expected for an ideal system is measured, but for high magnetic fields the measured gap approaches the bare Landau-level separation. Since the results at $\nu = 6$ show that the $N = 1$ Landau level behaves as expected, this peculiar behavior at $\nu = \pm 2$ can only be explained by the unique nature of the $N = 0$ Landau level shared equally between electrons and holes of opposite chirality.

In order understand this behavior in more detail we have to consider that the measured activation gap is determined by the distance from the chemical potential to the conductivity edges of the two adjacent Landau levels. When these levels have considerably different mobilities or widths (a case normally not encountered in traditional QHE samples), this gap will be dominated by the distance of the Fermi energy to the nearest Landau level with the highest mobility minus half its width. Therefore, in our case the conductivity around $\nu = 2$ is dominated by thermal excitation to the $N = 0$ Landau level since the peak conductivity measured in density sweeps is considerably larger for the $N = 0$ Landau level than for $N = 1$ [see Fig. 1(e)]. In particular, when this level is narrow enough, the high field excitation gap then just reflects the bare Landau-level separation.

Such a narrowing of the lowest Landau level is also supported theoretically by the following arguments: a major source of disorder in graphene can be tracked down to its corrugated (rippled) surface structure [25–28] leading to random fluctuations of the perpendicular magnetic field and, as a consequence, a considerable broadening of higher Landau levels. The zero-energy level, however, is exceptional in this sense. It is topologically protected by the so-called Atiyah-Singer index theorem, such that the number of states with zero energy is only determined by the total magnetic flux through the system and does not depend on whether this field is uniform or not [8,11]. Therefore, the fluctuations of the vector potential caused by ripples are not able to broaden this zero-energy state. The special nature of this state is most pronounced in high magnetic fields where the lowest Landau level is well separated form the neighboring levels; for lower fields Landau-level mixing can broaden the lowest Landau level by means of inter-Landau-level scattering.

For a more quantitative analysis we estimate the density of states in the higher Landau levels $N = 1$ and $N = 2$ from the measured resistivity as a function of concentration. Identifying localized states with a zero low-temperature resistivity ρ_{xx} and extended states with non-

zero ρ_{xx} we find that the number of localized states between the first and second Landau level is about 2.5 times the number of extended states in one of the levels. Knowing the width of the extended states $\Gamma = 400$ K, as deduced above, the form of the first and second Landau level is fully determined and quantitatively sketched in the inset of Fig. 3(c).

Using this density of states for the $N = 1$ level and a sharp $N = 0$ level allows us to calculate the field and temperature dependence of the chemical potential ϵ_F at $\nu = \pm 2$ using standard Fermi statistics. Above 100 K and in high magnetic fields ϵ_F is found to be near the middle of the gap. The conductivity at $\nu = \pm 2$ is then dominated by thermal excitation to the $N = 0$ Landau level (with the highest mobility) which amount to half the Landau-level distance, a value we indeed measure experimentally. These findings also agree with our Arrhenius plots in Fig. 2 with a well-defined single slope for $T > 100$ K.

Interestingly, our proposed scenario of an asymmetric density of states around $\nu = 2$ also implies a reduction of the Arrhenius slope for $T < 100$ K. It forces the Fermi energy ϵ_F to move from a midgap position closer towards the lowest Landau level. This effect indeed reduces the low-temperature activation energies and is independent from other effects such as variable-range hopping which can play a similarly important role for the reduction of the measured gaps.

Finally, we note that the measured gaps are extremely sensitive to background doping from surface impurities. Exposing the sample to air, hereby absorbing surface impurities, induces extra doping and considerably reduces the measured gaps. In particular, a narrowing of the lowest Landau level can no longer be observed. This statement is also confirmed by the fact that the strong temperature dependence of the $\nu = 2$ gap disappears for a system with surface impurities.

In conclusion, we have measured the excitation gaps at $\nu = \pm 2$ and $\nu = 6$ in graphene. We have shown that the results for higher Landau levels can be described quantitatively by thermal activation to broadened Landau levels with a large Landau-level width $\Gamma \approx 400$ K for the sample investigated. The lowest Landau level, however, becomes very sharp with increasing magnetic field, and the gap approaches the bare Landau-level splitting.

Part of this work has been supported by EuroMagNET under EU Contract No. RII3-CT-2004-506239 and by the Stichting Fundamenteel Onderzoek der Materie (FOM) with financial support from the Nederlandse Organisatie voor Wetenschappelijk Onderzoek (NWO).

*J.Giesbers@science.ru.nl
†U.Zeitler@science.ru.nl

[1] K. v. Klitzing, G. Dorda, and M. Pepper, Phys. Rev. Lett. **45**, 494 (1980).
[2] See, e.g., D. Yoshioka, *The Quantum Hall Effect* (Springer, New York, 2002).
[3] B. Jeckelmann and B. Jeanneret, Rep. Prog. Phys. **64**, 1603 (2001).
[4] K. S. Novoselov *et al.*, Science **306**, 666 (2004).
[5] K. S. Novoselov *et al.*, Proc. Natl. Acad. Sci. U.S.A. **102**, 10 451 (2005).
[6] Y. Zhang *et al.*, Phys. Rev. Lett. **96**, 136806 (2006).
[7] A. K. Geim and K. S. Novoselov, Nat. Mater. **6**, 183 (2007).
[8] M. I. Katsnelson, Mater. Today **10**, 20 (2007).
[9] G. W. Semenoff, Phys. Rev. Lett. **53**, 2449 (1984).
[10] F. D. M. Haldane, Phys. Rev. Lett. **61**, 2015 (1988).
[11] K. S. Novoselov *et al.*, Nature (London) **438**, 197 (2005).
[12] Y. Zhang, Y. Tan, H. L. Stormer, and P. Kim, Nature (London) **438**, 201 (2005).
[13] V. P. Gusynin and S. G. Sharapov, Phys. Rev. Lett. **95**, 146801 (2005).
[14] N. M. R. Peres, F. Guinea, and A. H. Castro Neto, Phys. Rev. B **73**, 125411 (2006).
[15] K. S. Novoselov *et al.*, Nature Phys. **2**, 177 (2006).
[16] E. McCann and V. I. Falko, Phys. Rev. Lett. **96**, 086805 (2006).
[17] K. S. Novoselov *et al.*, Science **315**, 1379 (2007).
[18] F. Schedin *et al.*, Nat. Mater. **6**, 652 (2007).
[19] D. A. Abanin *et al.*, Phys. Rev. Lett. **98**, 196806 (2007).
[20] K. Nomura and A. H. MacDonald, Phys. Rev. Lett. **96**, 256602 (2006).
[21] The gaps at $\nu = 6$ were measured in two different cooldowns; as a result the 25 and 30 T lines in Fig. 3(b) are slightly shifted upwards. In order to confirm that the measured gaps at high fields were still in agreement with the rest of the measurements, we compared the gap at 15 and 20 T for both cooldowns and found that they showed an almost identical value.
[22] Y. Ono *et al.*, J. Phys. Soc. Jpn. **51**, 237 (1982).
[23] G. Ebert *et al.*, Solid State Commun. **45**, 625 (1983).
[24] T. Ando, A. B. Fowler, and F. Stern, Rev. Mod. Phys. **54**, 437 (1982).
[25] S. V. Morozov *et al.*, Phys. Rev. Lett. **97**, 016801 (2006).
[26] J. C. Meyer *et al.*, Nature (London) **446**, 60 (2007); Solid State Commun. **143**, 101 (2007).
[27] E. Stolyarova *et al.*, Proc. Natl. Acad. Sci. U.S.A. **104**, 9209 (2007).
[28] M. I. Katsnelson and K. S. Novoselov, Solid State Commun. **143**, 3 (2007).